World Journal of Surgical Oncology

RESEARCH

Open Access

Anlotinib inhibits c-MET and ITGA2 in the treatment of anaplastic thyroid carcinoma

Shunshun Zhao[1†], Mingyao Meng[2,3†], Ruochuan Cheng[1], Min Zhang[1], Chuanyuan Liu[1], Qiuyu Meng[1], Tingting Yang[1], Haohan Huang[1], Bin Liu[1], Xiaodan Wang[2,3*] and Yanjun Su[1*]

Abstract

Objective This study explored the therapeutic effects of anlotinib in anaplastic thyroid carcinoma (ATC) models and the underlying molecular mechanisms.

Methods Human C643 and CAL-62 anaplastic thyroid carcinoma cell lines were cultured in vitro and treated with anlotinib. The effects of anlotinib on the proliferation, apoptosis, cell cycle progression, migration, and invasion of C643 and CAL-62 cells were observed. The tumour volumes and body weights of BALB/c-nu mice bearing subcutaneous tumours were recorded within 14 days of anlotinib treatment. HE staining and immunohistochemical staining for Ki67 and CD31 were performed on the tumour tissues from the mice. We collected anlotinib-treated and untreated C643 cell samples for subsequent transcriptome sequencing and analysis. Western blotting was conducted to measure the protein expression of c-MET, p-MET, LAMC2, COL5A1, and ITGA2 in mouse tumour tissues and C643 cell samples.

Results Anlotinib inhibited the growth of C643 and CAL-62 cells in a dose-dependent manner. Anlotinib also induced apoptosis and caused cell cycle arrest at the G2/M phase in C643 and CAL-62 cells ($p < 0.05$). Anlotinib significantly reduced the migration and invasion of C643 and CAL-62 cells ($p < 0.001$). Moreover, anlotinib effectively suppressed the growth of subcutaneously transplanted tumours in mice ($p < 0.05$). Immunohistochemical staining for Ki67 and CD31 demonstrated that anlotinib significantly inhibited tumour cell proliferation and angiogenesis. Furthermore, anlotinib downregulated the protein expression of p-MET, LAMC2, COL5A1, and ITGA2 in mouse tumour tissues and C643 cells ($p < 0.05$).

Conclusion This study confirmed the therapeutic effect of anlotinib on ATC via in vivo and in vitro experiments. In addition, preliminary studies suggest that the mechanism of anlotinib in treating ATC may be to alter the high invasiveness of ATC cells by inhibiting c-MET signaling pathway.

Keywords Anlotinib, Anaplastic thyroid carcinoma, c-MET, ITGA2, COL5A1

†Shunshun Zhao is the first author.

†Mingyao Meng is the co-first author.

*Correspondence:
Xiaodan Wang
wxdky001@163.com

Yanjun Su
suyanjun20042003@aliyun.com
[1]The First Affiliated Hospital of Kunming Medical University, 295 Xichang Road, Kunming 650032, China
[2]Yan'an Hospital Affiliated to Kunming Medical University, 245 people's East Road, Kunming 650051, China
[3]Key Laboratory of Tumor Immunological Prevention and Treatment of Yunnan Province, Kunming 650051, China

Introduction

Thyroid cancer is the most common malignant tumour that affects the endocrine system [1]. It is classified into four subtypes: papillary thyroid carcinoma (PTC), follicular thyroid carcinoma (FTC), medullary thyroid carcinoma (MTC), and anaplastic thyroid carcinoma (ATC). The first two are collectively termed differentiated thyroid carcinoma (DTC). Although the incidence of ATC is low in thyroid cancer patients, it is the most malignant thyroid cancer subtype and the main cause of death from thyroid cancer. The prognosis of ATC is very poor with the median survival time being only 3–7 months, and only approximately 20% of patients survive for more than one year [1–3]. ATC is extremely invasive, and its clinical manifestations include rapid tumour growth, tumour infiltration, and adjacent tissue compression. Approximately half of all ATC patients already have distant metastases at the time of definitive diagnosis, and the lung is the most common metastatic site, accounting for approximately 78% of metastatic cases [4–6]. Traditional treatment methods, such as surgery, radiotherapy, and chemotherapy, have little effect [3]. Therefore, new treatment strategies are urgently needed.

At present, a variety of molecular targeted drugs are known to be applied clinically, among which tyrosine kinase inhibitors (TKIs) are the most widely used inhibitors in the treatment of thyroid cancer [7]. Anlotinib is a novel small molecule multitarget TKI that has been used in the clinical treatment of MTC. For patients with radioactive iodine-refractory differentiated thyroid carcinoma (RAIR-DTC), studies have demonstrated that anlotinib significantly prolongs progression-free survival (PFS) in those with locally advanced or metastatic RAIR-DTC [8, 9]. However, there are only a few studies on the treatment of ATC with anlotinib. Retrospective clinical studies suggest that ATC patients may benefit from TKI treatment [10]. In addition, there have been study reported in which anlotinib combined with other drugs has been used to treat ATC [11]. For ATC, which is most aggressive histopathology type of thyroid cancer, combination therapy may be the future direction of treatment. Further basic research to explore the molecular mechanism of anlotinib in the treatment of ATC will provide theoretical basis for future clinical combination drug selection.

In this study, a human ATC cell line and a subcutaneous transplantation model in nude mice were selected as the research objects, and the therapeutic effect of anlotinib on ATC and the possible molecular mechanism involved were explored through in vivo and in vitro experiments, with the aim of providing theoretical support for the clinical treatment of ATC with anlotinib.

Materials and methods

Compounds

Anlotinib was obtained from Zhengda Tianqing Pharmaceutical Group Co., Ltd. The drug was dissolved in dimethyl sulfoxide (DMSO, Sigma) and stored at -20 °C. Then, it was diluted with phosphate-buffered saline (PBS, Vivacell) or culture medium to the desired concentration for in vivo and in vitro experimental studies. The final DMSO concentration in all working solutions was carefully maintained at less than 0.1%.

Cell lines and cell culture

The two human ATC cell lines used in this study, C643 and CAL-62, were purchased from the American Type Culture Collection (ATCC) (Manassas, VA, USA). C643 cells were cultured in growth medium consisting of 90% RPMI-1640 (Gibco), 10% FBS (Gibco), 2 mM L-glutamine, and 5000 units/mL penicillin and streptomycin. CAL-62 cells were cultured in growth medium consisting of 90% DMEM (high glucose, Vivacell), 10% FBS, 2 mM L-glutamine, and 5000 units/mL penicillin and streptomycin. The cells were cultured in a chamber with 5% CO_2 at 37 °C and maintained in the exponential phase of growth during all the experiments.

Cell viability and cell proliferation assay

A CCK-8 assay was used to explore the effect of anlotinib on ATC cell viability. Cells (C643 or CAL-62 cells) were seeded in 96-well plates with 5000 cells per well. Five replicate wells were established for each group. After incubation for 24 h, 100 µl of complete medium containing 0, 0.5, 1, 2, 5, 10, 20, or 40 µmol/L anlotinib was added to each well for each group, and the incubation was continued at 37 °C for 24 h. At the appropriate times, the anlotinib solution in each well was replaced with 100 µl of CCK-8 diluted in complete medium and incubated for 1.5 h at 37 °C. Finally, the OD value was measured with a spectrophotometer at 450 nm. The median inhibitory concentration (IC50 value) was calculated using the Four - parameter logistic model in Prism 9.0 software (GraphPad Software). In addition to five technical replicate wells per group, a total of three independent biological replicates were conducted using distinct cell batches on separate experimental days to assess reproducibility.

Cell cycle analysis

Cells were treated with complete medium containing the appropriate concentrations of anlotinib (C643 cells: 0 µmol/L, 7 µmol/L) for 48 h. The treated cells were collected and fixed with prechilled 75% ethanol at 4 °C overnight. The cells were labelled with a cell cycle detection kit (no. C1052; Beyotime, Shanghai, China). The samples were analysed with a FACS Calibur flow cytometer (BD

Biosciences). Each experiment was performed three independent times.

Cell apoptosis analysis

C643 or CAL-62 cells in the logarithmic phase of growth were seeded in 6-well plates, laying 4×10^5 cells per well. After the cells had completely attached to the well, they were treated with complete medium containing different concentrations of anlotinib (C643 cells: 0,7 μmol/L; CAL-62 cells: 0,5 μmol/L) for 24 h. The cells were subsequently collected, and apoptosis was assessed with an Annexin V apoptosis detection kit (eBioscience, United States). The stained cells were analysed with a FACS Calibur flow cytometer (BD Biosciences). Data were obtained from three independent experiments.

Wound healing assay

Cells in the logarithmic phase of growth (C643 or CAL-62) were seeded at a density of 4×10^5 cells per well in a 6-well plate and allowed to grow into a confluent monolayer. A line was gently drawn in the cell monolayer with a p200 pipette tip. The culture plate was rinsed with PBS 2–3 times to remove the detached cells. Each group was treated with serum-free culture medium containing the corresponding concentration of anlotinib (C643 cells: 0, 7 μmol/L; CAL-62 cells: 0, 5 μmol/L). The plate was then placed in a 37 °C incubator for culture. Samples were subsequently collected at 0 h and 24 h and photographed under an inverted microscope. Cell migration was quantitatively analysed with ImageJ software. The experiment was repeated three times.

Invasion assay

Cell samples were separately collected from the anlotinib and control groups and resuspended in serum-free medium. An invasion assay was performed using a 24-well Transwell plate (Corning). Two hundred microlitres of cell suspension was added to the upper chamber, and 500 μL of complete medium was added to the lower chamber. After 48 h of culture, the cells were fixed with 4% formaldehyde solution (Servicebio) for 10–15 min and then stained with 0.1% crystal violet (Servicebio) for 8 min. Finally, the cells in 5 fields were observed and counted under a microscope, and the average value was taken. Data are from three independent experiments.

In vivo subcutaneous tumour model (tumorigenicity study of C643 cells)

The experimental animals that were used in this study were 4-week-old female BALB/c-nu nude mice, weighing between 18 and 20 g, and they were obtained from Beijing Sibeifu Biotechnology Co., Ltd. (Beijing, China). The BALB/c-nu nude mice were maintained in a specific pathogen-free (SPF) environment at the Animal Experiment Center of Kunming Medical University. All the animal experiments were approved by the Animal Experiment Ethics Review Committee of Kunming Medical University (Approval number: kmmu20231505), and the animals were humanely cared for according to the standards of the Guide for the Care and Use of Laboratory Animals. C643 cells were harvested during the logarithmic phase of growth and resuspended in precooled PBS. The final cell concentration was adjusted to 3×10^7/ml. Subsequently, 100 μl of the cell suspension was subcutaneously injected into the right nape of each nude mouse. Tumour growth was observed and recorded at regular intervals. Once the tumour volume reached approximately 50–100 mm^3, the mice were randomly assigned to either the control group ($n = 8$) or the anlotinib group ($n = 8$). The nude mice in the control and anlotinib groups were administered an equal volume of dimethyl sulfoxide (DMSO)-containing PBS (100 μl/d) and anlotinib diluted in PBS (6 mg/kg, 100 μl/d), respectively, via daily intraperitoneal injection for a period of two weeks. During this period, the dimensions of the tumours and the body weights of the mice were recorded at 3-day intervals. To ensure the integrity of the data, we implemented a double - blind protocol. The individuals who administered the treatments were different from those who measured the tumors. After two weeks, the mice were euthanized by cervical dislocation, and the tumour tissue was harvested for subsequent analyses.

Haematoxylin–eosin (HE) staining and immunohistochemistry (IHC)

The tumour tissues were fixed in 4% paraformaldehyde, embedded in paraffin, and cut into 4–5 μm thick sections. The sections were then stained with haematoxylin and eosin (HE). Immunohistochemistry (IHC) was performed according to standard procedures, and the results were visualized with DAB reagent. The antibodies used IHC were anti-Ki67 (Proteintech) and anti-CD31 (Proteintech) antibodies. Images were captured with a light microscope.

RNA sequencing (RNA-seq)

C643 cell samples were separately collected from the anlotinib and the control groups. Chongqing Life Knowledge Source Technology Co., Ltd. was then commissioned to perform transcriptomic sequencing analysis on the samples. They employed the Illumina HiSeq platform, renowned for its high-throughput capabilities and reliable sequencing outcomes, which guaranteed the quality of our data. For the differential gene expression criteria, we established a log2 fold-change cutoff of > 1 or < -1, in conjunction with an adjusted P-value of < 0.05.

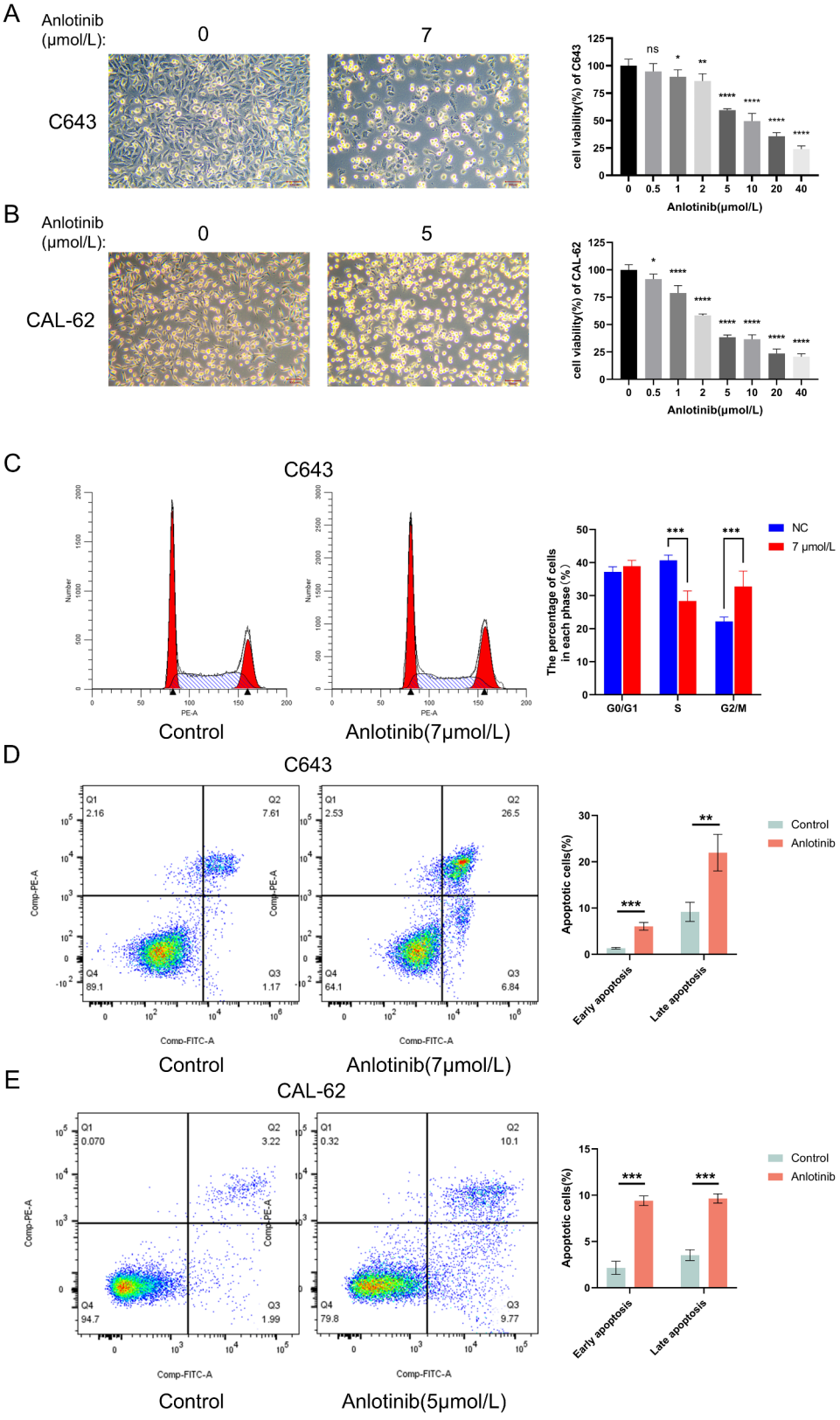

Fig. 1 (See legend on next page.)

(See figure on previous page.)

Fig. 1 Anlotinib can inhibit the growth of ATC cells, block cell cycle progression at the G2/M phase, and induce apoptosis. (**A** and **B**) C643 and CAL-62 cells cultured in vitro were treated with anlotinib (0, 0.5, 1, 2, 5, 10, 20, and 40 μmol/L). After 24 h, cell viability was determined via the CCK-8 assay, and the cells were observed and images were captured under an inverted microscope. Scale bar: 100 μm. (**C**) C643 cells were treated with anlotinib (0.7 μmol/L) for 24 h in vitro, stained with PI, analysed by flow cytometry, and quantified via ModFit software. (**D** and **E**) C643 (**D**) and CAL-62 (**E**) cells were treated with anlotinib for 24 h in vitro, stained with Annexin V-FITC/PI, analysed by flow cytometry, and analysed via FlowJo software. Upper left quadrant (Q1): Mechanically injured cells, upper right quadrant (Q2): late apoptotic cells, lower right quadrant (Q3): early apoptotic cells, lower left quadrant (Q4): normal cells. All the data were obtained from three independent experiments. * $p < 0.05$, ** $p < 0.01$, *** $p < 0.001$, **** $p < 0.0001$

Western blotting analysis

ATC cells and nude mouse tumour tissues were treated with RIPA lysis buffer (Beyotime) supplemented with protease and phosphatase inhibitors. The protein concentration was determined with a BCA protein assay kit (Beyotime) to ensure equal protein loading across samples. Specifically, equal amounts of protein were loaded for both the anlotinib - treated group and the control group. Proteins were separated by 10% SDS–PAGE and transferred to PVDF membranes (Millipore). The membranes were probed with specific antibodies. The primary antibodies used were specific for c-MET (Cell Signaling Technology,1:1000), p-MET (Cell Signaling Technology,1:1000), LAMC2 (Santa Cruz,1:100), COL5A1 (Santa Cruz,1:100), ITGA2 (Abcam,1:5000), and GAPDH (Proteintech,1:5000), with GAPDH serving as the protein loading control. The membranes were incubated with these primary antibodies at 4 °C on a shaker overnight. The next day, the membranes were incubated with secondary antibodies, including goat anti-rabbit or anti-mouse horseradish peroxidase-conjugated IgG (Proteintech,1:5000), for 1 h at room temperature. Finally, the target proteins were visualized via ECL Plus (Proteintech) and an enhanced chemiluminescence detection system (Bio-Rad).

Statistical analysis

The data analysis was conducted using SPSS 22.0 software, while GraphPad Prism 9 software was employed for graph creation. The data are presented as mean ± standard deviation, and comparisons were made using a Student's t-test for two groups, or one-way ANOVA for multiple groups. A P-value of < 0.05 was considered statistically significant.

Results

Anlotinib inhibits proliferation and induces apoptosis and cell cycle arrest at the G2/M phase in human ATC cells in vitro

We incubated ATC cell lines (C643 and CAL-62 cells) with media supplemented with different concentrations of anlotinib (0, 0.5, 1, 2, 5, 10, 20, or 40 μmol/L) for 24 h and used a CCK8 assay to assess the viability of the tumour cells; the results revealed that anlotinib significantly inhibited the growth of the tumour cells in a dose-dependent manner (Fig. 1. A–B). The IC50 values of anlotinib in C643 and CAL-62 cells were 6.573 and 4.170, respectively, after 24 h. Flow cytometry was used to evaluate cell cycle progression and tumour cell apoptosis. Cell cycle analysis revealed that anlotinib induced cell cycle arrest in the G2/M phase in C643 cells (Fig. 1C). The rate of C643 and CAL-62 cell apoptosis was significantly increased after anlotinib administration (Fig. 1D–E).

Anlotinib inhibits the migration and invasion of human ATC cells in vitro

The wound healing assay also revealed a significant decrease in the migration of cancer cells after 24 h of anlotinib treatment (Fig. 2A–B). The results of the cell invasion experiments indicated that the invasion of these two undifferentiated thyroid cancer cell lines was significantly inhibited after treatment with anlotinib (Fig. 2C-D). These findings suggest that anlotinib can significantly inhibit the migration and invasion of undifferentiated thyroid cancer cells.

Anlotinib exhibited potent antitumour activity in vivo

We further explored the effect of anlotinib in vivo. Tumour growth was rapid and significant in the control mice (Fig. 3A and C), and the tumour weight in the control group was significantly greater than that in the anlotinib-treated group (Fig. 3B). We found that administering anlotinib for 14 days had no significant effect on the body weights of the mice (Fig. 3D). There were also no alterations in diarrhoea, appetite, or mental status following anlotinib administration. Histopathological examination (HE) of the tumour tissues revealed the presence of many heterogeneous tumour cells. Immunohistochemical (IHC) assays revealed that anlotinib treatment inhibited the expression of Ki67 and CD31 (Fig. 3E). In conclusion, these results strongly indicate the potent antitumour activity of anlotinib in vivo.

Anlotinib improves ATC by inhibiting the c-MET signaling pathway

Transcriptome sequencing of anlotinib-treated and untreated C643 cell samples revealed that differentially expressed genes were significantly enriched in signaling pathways such as MET promotes cell motility and Extracellular matrix organization. Moreover, the differentially expressed genes mostly included the LAMC2, COL5A1and ITGA2 genes, which are related to the MET

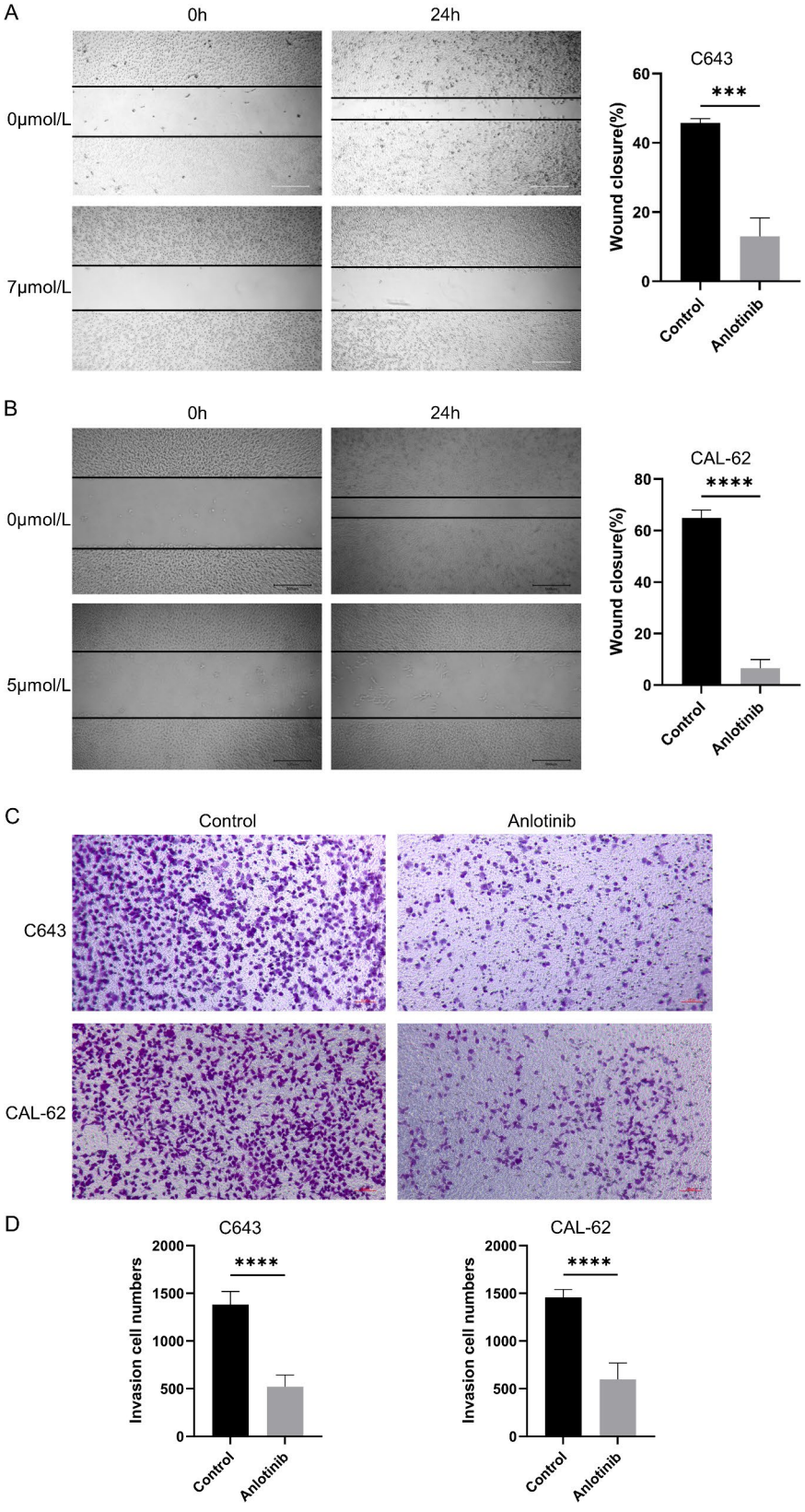

Fig. 2 (See legend on next page.)

(See figure on previous page.)

Fig. 2 Anlotinib can inhibit the migration and invasion of ATC cells. (**A** and **B**) ATC cells cultured in vitro were treated with anlotinib (for C643 cells: 0, 7 μmol/L; for CAL-62 cells: 0, 5 μmol/L). An inverted microscope was used to observe and image the cells at 0 h and 24 h to determine the effect of anlotinib on the migration of ATC cells. Scale bar: 500 μm. (**C** and **D**) ATC cells cultured in vitro were treated with anlotinib (for C643 cells: 0, 7 μmol/L; for CAL-62 cells: 0, 5 μmol/L). After 48 h, an inverted microscope was used to observe and record the effect of anlotinib on the invasion of ATC cells. Scale bar: 50 μm. All the data are from three independent experiments. *** $p < 0.001$, **** $p < 0.0001$

signaling pathway and Extracellular matrix organization (Fig. 4A-D).

In order to clarify the changes in the expression of MET signaling pathway and downstream proteins after anlotinib treatment, western blotting was used to detect the expression of c-MET, p-MET, LAMC2, COL5A1, and ITGA2 proteins in ATC cells and nude mouse tumour tissues.

The expression of c-MET, p-MET, LAMC2, COL5A1, and ITGA2 in ATC cells and subcutaneous tumour tissues was significantly upregulated, whereas the expression of these proteins was significantly inhibited after treatment with anlotinib (Fig. 4E-H). Our results suggest that anlotinib may exert antitumour effects on ATC by acting on the tyrosine kinase receptor c-MET, inhibiting the expression of c-MET-related signaling pathway proteins by decreasing its phosphorylation level.

Discussion

Our results revealed that anlotinib has a therapeutic effect on in vivo transplanted tumor models of ATC, which are consistent with Juyong Liang 's research [12]. In vitro experiments, we found that anlotinib significantly inhibited the proliferation of ATC cells, which is consistent with the results of Professor Gaoming's team [13]. More importantly, we found that anlotinib significantly inhibited the migration and invasion of ATC cells. ATC is a highly metastatic cancer with limited therapeutic alternatives. Recent studies have found that anlotinib can inhibit the proliferation of ATC and promote ferroptosis [14, 15]. No studies have explored the inhibitory effect of anlotinib on the invasion and migration of ATC cells, but this is a new finding in our study. However, due to the small number of cases in the clinical trials on the treatment of ATC with anlotinib [11], the situation of ATC metastasis has not been analyzed.

Anlotinib is a novel multi-target tyrosine kinase inhibitor that is designed to primarily inhibit VEGFR, FGFR, PDGFR, c-Kit, and Ret [16]. However, the targets of anlotinib treatment may vary for different tumors. Further exploration of the mechanism of anlotinib for ATC may provide a basis for combination therapy in ATC patients and a biomarker for suitable selection for clinical treatment. Through RNA sequencing and verification, we found that anlotinib exerts a therapeutic effect on ATC by inhibiting c-MET signaling pathway and downstream molecules LAMC2, COL5A1, and ITGA2.

C-MET is a member of the tyrosine kinase receptor family, which binds to the ligand hepatocyte growth factor (HGF) and activates several important signaling pathways to regulate the function of tumor cells, including survival, proliferation, and migration. C-MET has been shown to be overexpressed and/or mutated in a variety of malignancies and is associated with tumour cell invasion and metastasis [17–21]. Previous scholars have reported that c-MET is highly expressed in ATC cell lines, which is consistent with our research results [22]. Studies have reported that c-MET significantly increases the aggressiveness of ATC cells by promoting their motility and invasiveness [22–24].

Our study found that p-MET was significantly downregulated after anlotinib treatment, suggesting that anlotinib has an inhibitory effect on the tyrosine kinase c-MET. Gangyang Wang have also found that anlotinib can improve the situation in osteosarcoma by inhibiting c-MET [25]. In addition, Xiali Tang's study has found that anlotinib can inhibit the invasion and migration of the H466 cell of small cell lung cancer by suppressing c-MET [26]. Therefore, we believe that anlotinib may inhibit the invasiveness of ATC cells by suppressing c-MET signaling pathway. In recent years, an increasing number of studies have shown that the c-MET and integrin signaling systems have precise mutual regulatory effects [27]. Integrins directly bind c-MET and enhance its signaling to promote tumour invasion and metastasis [27, 28]. Some studies have found that c-MET/β1 integrin complex can induce bone metastasis of triple negative breast cancer [29, 30]. Our results also revealed that ITGA2 was significantly upregulated in ATC cells, which can be significantly inhibited by anlotinib treatment. ITGA2 is highly expressed in many malignant tumours and is closely related to lymph node and distant metastasis, and its expression level is positively correlated with tumour aggressiveness [31, 32].

Integrins are key mediators of cell migration, providing physical and biochemical links between the ECM and the cytoskeleton [33]. At present, it has not been reported that ITGA2 is involved in the invasion and metastasis of ATC, but some scholars have reported that ITGA2 forms an integrin heterodimer through noncovalent binding with the β1 subunit, which mediates the adhesion of cells to the ECM [27, 34, 35]. Other studies have shown that c-MET signal transduction requires integrin-mediated cell adhesion to the ECM to accelerate cell movement, thereby increasing the aggressiveness of tumour cells.

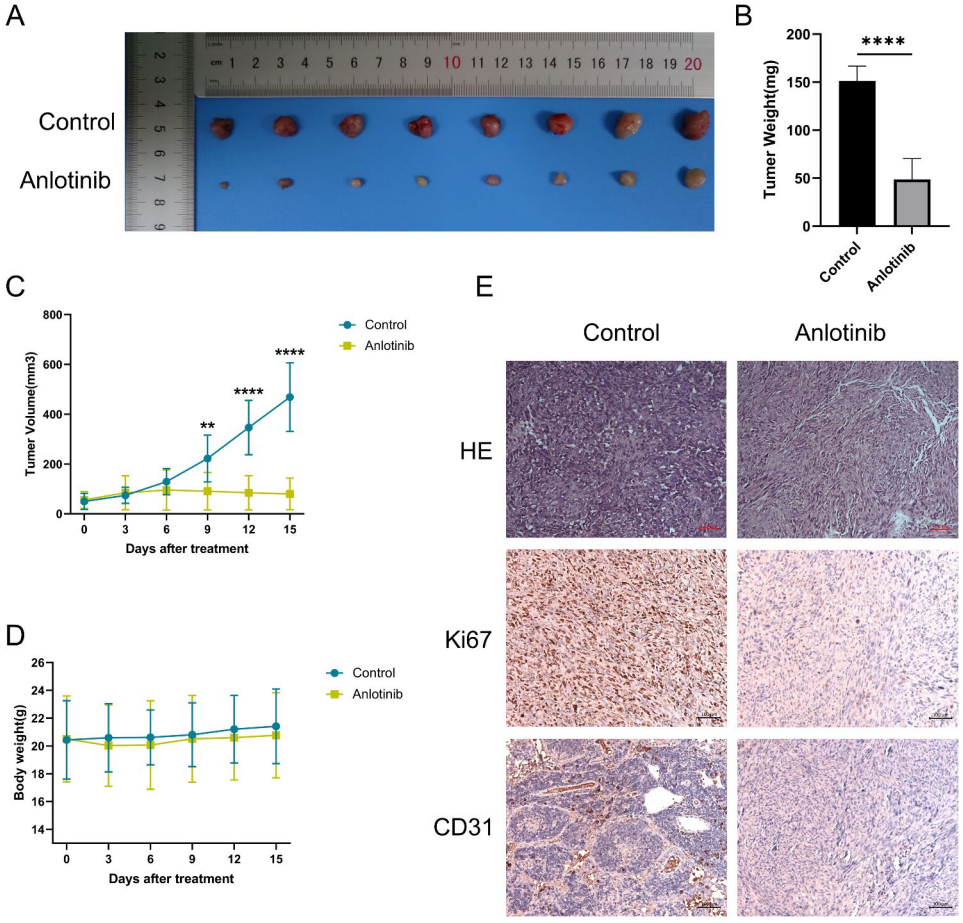

Fig. 3 Anlotinib can inhibit the growth of subcutaneous xenografts in nude mice. Nude mice in the control group ($n=8$) and the anlotinib group ($n=8$) were intraperitoneally injected with equal volumes of PBS containing dimethyl sulfoxide (100 µl/d) or anlotinib diluted with PBS (6 mg/kg, 100 µl/d), respectively. After 14 days of treatment, the nude mice were sacrificed by cervical dislocation, and the tumour tissues were removed. (**A**) Visual comparison of the size of tumour tissues in nude mice in the control group and the anlotinib group. (**B**) Quantitative comparison of the weights of the tumour tissues from the nude mice in the control and anlotinib groups. Comparison of the tumour volume (**C**) and body weight (**D**) of the nude mice during drug administration. (**E**) HE, Ki67, and CD31 IHC staining of tumour tissues with or without anlotinib treatment. Scale bar: 100 µm. ** $p<0.01$, **** $p<0.0001$

Glycoproteins in the extracellular matrix (ECM), including laminin and fibronectin, promote binding between c-MET and integrins, leading not only to ligand-independent activation of c-MET but also to amplification of signaling [36].

In addition to ITGA2, our in vivo and in vitro experiments also found that the expression of LAMC2 and COL5A1 was significantly inhibited by anlotinib treatment. Garg M et al. reported that LAMC2 was highly expressed in ATC tissues and cells compared with normal thyroid tissue. Silencing LAMC2 in ATC cells with shRNAs significantly reduced the growth of xenograft tumours in immunodeficient mice. LAMC2 gene knockdown leads to cell cycle arrest and significantly inhibits its ATC cell migration and invasion. Microarray data revealed that LAMC2 knockdown significantly altered the expression of genes related to migration, invasion, proliferation, and survival [37]. Researchers sequenced ATC cells and discovered five specific genes, including COL5A1, which is upregulated in ATC [38]. Some scholars have found that COL5A1 promotes metastasis of gastric cancer [39], but in thyroid cancer, there are only studies on the promotion of PTC metastasis by COL5A1 [40]. Our study suggests that COL5A1 is down-regulated after anlotinib treatment, and whether it is related to the inhibition of invasion needs follow-up research.In conclusion, Our experiments demonstrate that anlotinib has a therapeutic effect on ATC. Moreover, preliminary findings from transcriptome sequencing revealed that the mechanism of anlotinib in treating ATC may be to alter the high invasiveness of ATC cells by inhibiting c-MET signaling pathway. However, in this study, we did not knock down c-MET to verify the invasion of ATC cells and the therapeutic effect of anlotinib. Additionally, we have not fully elucidated the interaction between c-MET and ITGA2, as well as that between c-MET, LAMC2 and COL5A1. These are the limitations of this study, and further experiments are needed for in-depth research. In

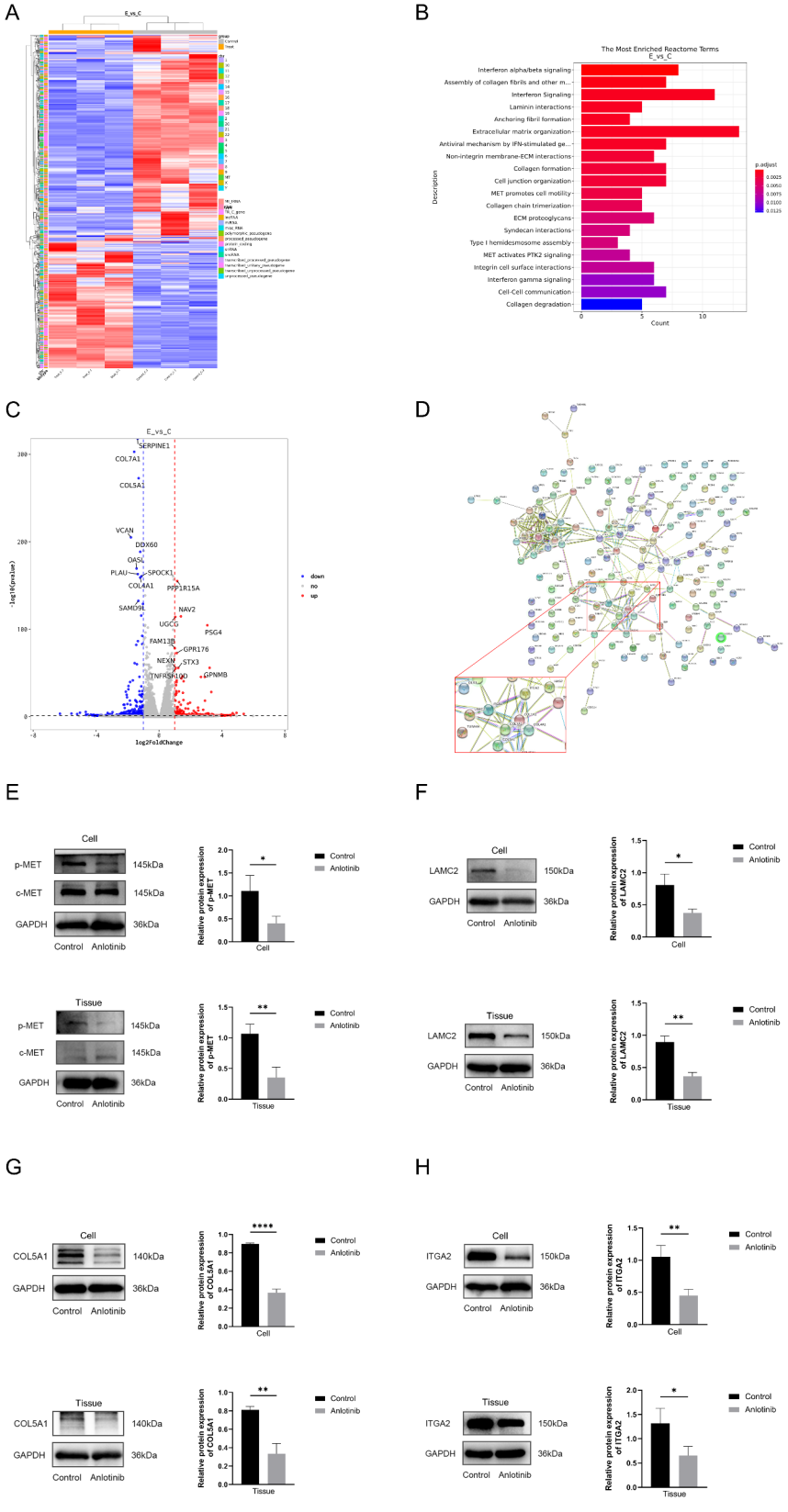

Fig. 4 (See legend on next page.)

(See figure on previous page.)

Fig. 4 Transcriptome sequencing results and the expression of differentially expressed proteins in vivo and in vitro. (**A**) Differential gene clustering heatmap. (**B**) Histogram of differential gene Reactome enrichment results. (**C**) Volcano plot of differentially expressed genes. (**D**) Protein–protein interaction network analysis diagram. (**E**) Effects of anlotinib on the protein expression of c-MET and p-MET in vivo and in vitro. (**F**) Effect of anlotinib on the protein expression of LAMC2 in vivo and in vitro. (**G**) Effect of anlotinib on the expression of COL5A1 in vivo and in vitro. (**H**) Effect of anlotinib on the protein expression of ITGA2 in vivo and in vitro. * $p < 0.05$, ** $p < 0.01$, **** $p < 0.0001$

the future, research on the association between c-MET expression in tumor tissues of ATC patients and ATC metastasis can be conducted. Whether c-MET can serve as a predictor for anlotinib treatment of ATC requires analysis through large-sample clinical studies.

Supplementary Information

The online version contains supplementary material available at https://doi.org/10.1186/s12957-025-03810-5.

Supplementary Material 1

Acknowledgements
We would like to express our sincere gratitude to the teams and individuals who supported this research.

Author contributions
YJS, XDW, MYM and RCC contributed to conception and design of the study. SSZ contributed to animal and cell experiments. MZ, TTY, QYM and BL contributed to animal experiments. HHH and CYL contributed to cell experiments. SSZ performed the statistical analysis. All authors contributed to manuscript revision, read, and approved the submitted version.

Funding
This work is supported by grants from Yunnan Provincial Science and Technology Department (No. 202301AY070001-047), Yunnan Academician and Expert Workstation, No.202205AF150023, Yunnan Fundamental Research Projects, China (Grant No.202201AS070068), Xingdian Talent Support Program and 535 Talent Project of First Affiliated Hospital of Kunming Medical University(No.2023535D07) and Yunnan Clinical Medical Center for Endocrine and Metabolic Diseases(No. YWLCYXZXXYS20221005).

Data availability
No datasets were generated or analysed during the current study.

Declarations

Ethics approval and consent to participate
All the animal experiments were approved by the Animal Experiment Ethics Review Committee of Kunming Medical University (Approval number: kmmu20231505), and the animals were humanely cared for according to the standards of the Guide for the Care and Use of Laboratory Animals.

Consent for publication
Not applicable.

Competing interests
The authors declare no competing interests.

Received: 24 January 2025 / Accepted: 13 April 2025
Published online: 25 April 2025

References

1. PAN Z, XU T, BAO L, et al. CREB3L1 promotes tumor growth and metastasis of anaplastic thyroid carcinoma by remodeling the tumor microenvironment [J]. Mol Cancer. 2022;21(1):190.
2. BIBLE K C KEBEBEWE, BRIERLEY J, et al. 2021 American thyroid association guidelines for management of patients with anaplastic thyroid Cancer [J]. Thyroid. 2021;31(3):337–86.
3. GUI L, LIU S, ZHANG Y, et al. A remarkable and durable response to sintilimab and anlotinib in the First-Line treatment of an anaplastic thyroid carcinoma without targetable genomic alterations: A case report [J]. Onco Targets Ther. 2021;14:2741–6.
4. HAHN S Y, SHIN JH. Description and comparison of the sonographic characteristics of poorly differentiated thyroid carcinoma and anaplastic thyroid carcinoma [J]. J Ultrasound Med. 2016;35(9):1873–9.
5. IYER PC, DADU R, FERRAROTTO R, et al. Real-World experience with targeted therapy for the treatment of anaplastic thyroid carcinoma [J]. Thyroid. 2018;28(1):79–87.
6. KELIL T, KERALIYA A R, HOWARD SA, et al. Current concepts in the molecular genetics and management of thyroid cancer: an update for radiologists [J]. Radiographics. 2016;36(5):1478–93.
7. HAUGEN B R, ALEXANDER E K, BIBLE K C, et al. 2015 American thyroid association management guidelines for adult patients with thyroid nodules and differentiated thyroid cancer: the American thyroid association guidelines task force on thyroid nodules and differentiated thyroid Cancer [J]. Thyroid. 2016;26(1):1–133.
8. SU Y, CHENG S, QIAN J, et al. Case report: anlotinib therapy in a patient with recurrent and metastatic RAIR-DTC harboring coexistent TERT promoter and BRAF(V600E) mutations [J]. Front Oncol. 2021;11:626076.
9. CHI Y, ZHENG X, ZHANG Y, et al. Anlotinib in locally advanced or metastatic Radioiodine-Refractory differentiated thyroid carcinoma: A randomized, Double-Blind, multicenter phase II trial [J]. Clin Cancer Res. 2023;29(20):4047–56.
10. MUNTEAN C, SOLOMON A, CIPAIAN R C et al. The efficacy and safety of anlotinib in the treatment of thyroid cancer: A systematic review [J]. J Clin Med, 2025, 14(2).
11. SONG Y, ZHANG Y, BAI Y, et al. Combination kinase inhibitors and immunotherapy for unresectable anaplastic thyroid carcinoma: A retrospective single-center study [J]. Oral Oncol. 2024;159:107067.
12. LIANG J, JIN Z, KUANG J, et al. The role of anlotinib-mediated EGFR Blockade in a positive feedback loop of CXCL11-EGF-EGFR signalling in anaplastic thyroid cancer angiogenesis [J]. Br J Cancer. 2021;125(3):390–401.
13. RUAN X, SHI X. Antitumor effects of anlotinib in thyroid cancer [J]. Endocr Relat Cancer. 2019;26(1):153–64.
14. WU J, LIANG J, LIU R et al. Autophagic Blockade potentiates anlotinib-mediated ferroptosis in anaplastic thyroid cancer [J]. Endocr Relat Cancer, 2023, 30(9).
15. WU J, LIANG J, LIU R et al. ERRATUM: autophagic Blockade potentiates anlotinib-mediated ferroptosis in anaplastic thyroid cancer [J]. Endocr Relat Cancer, 2025, 32(2).
16. SUN Y, NIU W. Safety, pharmacokinetics, and antitumor properties of anlotinib, an oral multi-target tyrosine kinase inhibitor, in patients with advanced refractory solid tumors [J]. J Hematol Oncol. 2016;9(1):105.
17. ZAMBELLI A, BIAMONTI G. HGF/c-Met signalling in the tumor microenvironment [J]. Adv Exp Med Biol. 2021;1270:31–44.
18. NARDONE HC, ZIOBER A F, LIVOLSI V A, et al. c-Met expression in tall cell variant papillary carcinoma of the thyroid [J]. Cancer. 2003;98(7):1386–93.
19. RUCO L. The pathogenetic role of the HGF/c-Met system in papillary carcinoma of the thyroid [J]. Biomedicines. 2014;2(4):263–74.
20. YANG X, LIAO H Y, ZHANG HH. Roles of MET in human cancer [J]. Clin Chim Acta. 2022;525:69–83.
21. MA PC, MAULIK G, CHRISTENSEN J, et al. c-Met: structure, functions and potential for therapeutic Inhibition [J]. Cancer Metastasis Rev. 2003;22(4):309–25.
22. LEE K, LEE SH, KIM W, et al. Dsg2-mediated c-Met activation in anaplastic thyroid cancer motility and invasion [J]. Endocr Relat Cancer. 2020;27(11):601–14.
23. BERGSTRöM JD, DIAZ DE STåHL HERMANSSONA. Non-autocrine, constitutive activation of Met in human anaplastic thyroid carcinoma cells in culture [J]. Br J Cancer. 1999;80(5–6):650–6.

24. WILLIAMSON A J, DOSCAS M E, YE J, et al. The Sonic Hedgehog signaling pathway stimulates anaplastic thyroid cancer cell motility and invasiveness by activating Akt and c-Met [J]. Oncotarget. 2016;7(9):10472–85.
25. WANG G, SUN M, JIANG Y, et al. Anlotinib, a novel small molecular tyrosine kinase inhibitor, suppresses growth and metastasis via dual Blockade of VEGFR2 and MET in osteosarcoma [J]. Int J Cancer. 2019;145(4):979–93.
26. TANG X, ZHENG Y. Anlotinib inhibits cell proliferation, migration and invasion via suppression of c-Met pathway and activation of ERK1/2 pathway in H446 cells [J]. Anticancer Agents Med Chem. 2021;21(6):747–55.
27. STANISLOVAS J. c-Met-integrin cooperation: mechanisms, tumorigenic effects, and therapeutic relevance [J]. Front Cell Dev Biol. 2022;10:994528.
28. CHASTNEY M R, KAIVOLA J, LEPPäNEN VM, et al. The role and regulation of integrins in cell migration and invasion [J]. Nat Rev Mol Cell Biol. 2025;26(2):147–67.
29. JAHANGIRI A, NGUYEN A, CHANDRA A, et al. Cross-activating c-Met/β1 integrin complex drives metastasis and invasive resistance in cancer [J]. Proc Natl Acad Sci U S A. 2017;114(41):E8685–94.
30. LAU D, WADHWA H. SUDHIR S, Role of c-Met/β1 integrin complex in the metastatic cascade in breast cancer [J]. JCI Insight, 2021, 6(12).
31. DONG J, WANG R, REN G, et al. HMGA2-FOXL2 Axis regulates metastases and Epithelial-to-Mesenchymal transition of chemoresistant gastric Cancer [J]. Clin Cancer Res. 2017;23(13):3461–73.
32. MA L, SUN Y, LI D, et al. Overexpressed ITGA2 contributes to Paclitaxel resistance by ovarian cancer cells through the activation of the AKT/FoxO1 pathway [J]. Aging. 2020;12(6):5336–51.
33. CHASTNEY M R, KAIVOLA J, LEPPäNEN VM et al. The role and regulation of integrins in cell migration and invasion [J]. Nat Rev Mol Cell Biol, 2024.
34. ZHANG L, HUANG Y, LING J, et al. Is integrin subunit alpha 2 expression a prognostic factor for liver carcinoma?? A validation experiment based on bioinformatics analysis [J]. Pathol Oncol Res. 2019;25(4):1545–52.
35. GONG J, LU X, XU J, et al. Coexpression of UCA1 and ITGA2 in pancreatic cancer cells target the expression of miR-107 through focal adhesion pathway [J]. J Cell Physiol. 2019;234(8):12884–96.
36. DE HERDT M J, BAATENBURG DE JONG R J. HGF and c-MET as potential orchestrators of invasive growth in head and neck squamous cell carcinoma [J]. Front Biosci. 2008;13:2516–26.
37. GARG M, KANOJIA D, OKAMOTO R, et al. Laminin-5γ-2 (LAMC2) is highly expressed in anaplastic thyroid carcinoma and is associated with tumor progression, migration, and invasion by modulating signaling of EGFR [J]. J Clin Endocrinol Metab. 2014;99(1):E62–72.
38. ZHANG L, XU M, ZHANG W, et al. Three-dimensional genome landscape comprehensively reveals patterns of Spatial gene regulation in papillary and anaplastic thyroid cancers: a study using representative cell lines for each cancer type [J]. Cell Mol Biol Lett. 2023;28(1):1.
39. ZHANG Y, JING Y, WANG Y, et al. NAT10 promotes gastric cancer metastasis via N4-acetylated COL5A1 [J]. Signal Transduct Target Ther. 2021;6(1):173.
40. WANG C, WANG Y, FU Z, et al. MiR-29b-3p inhibits migration and invasion of papillary thyroid carcinoma by downregulating COL1A1 and COL5A1 [J]. Front Oncol. 2022;12:837581.

Publisher's note